Antiviral Research 105 (2014) 26–31

Contents lists available at ScienceDirect

Antiviral Research

journal homepage: www.elsevier.com/locate/antiviral

A murine model of coxsackievirus A16 infection for anti-viral evaluation

Qingwei Liu [1], Jinping Shi [1], Xulin Huang, Fei Liu, Yicun Cai, Ke Lan, Zhong Huang *

Center for Vaccine Sciences, Key Laboratory of Molecular Virology & Immunology, Institut Pasteur of Shanghai, Shanghai Institutes for Biological Sciences, Chinese Academy of Sciences, Shanghai, China

ARTICLE INFO

Article history:
Received 21 December 2013
Revised 13 February 2014
Accepted 17 February 2014
Available online 26 February 2014

Keywords:
Coxsackievirus A16
Infection
Murine model
Monoclonal antibody

ABSTRACT

Coxsackievirus A16 (CA16) is one of the main causative agents of hand, foot and mouth disease (HFMD), which is a common infectious disease in children. CA16 infection may lead to severe nervous system damage and even death in humans. However, study of the pathogenesis of CA16 infection and development of vaccines and anti-viral agents are hindered partly by the lack of an appropriate small animal model. In the present study, we developed and characterized a murine model of CA16 infection. We show that neonatal mice are susceptible to CA16 infection via intraperitoneal inoculation. One-day-old mice infected with 2×10^6 TCID50 of CA16/SZ05 strain consistently exhibited clinical signs, including reduced mobility, and limb weakness and paralysis. About 57% of the mice died within 14 days after infection. Significant damage in the brainstem, limb muscles and intestines of the infected mice in the moribund state was observed by histological examination, and the presence of CA16 in neurons of the brainstem was demonstrated by immunohistochemical staining with a CA16-specific polyclonal antibody, strongly suggesting the involvement of the central nervous system in CA16 infection. Analysis of virus titers in various organs/tissues collected at 3, 6 and 9 days post-infection, showed that skeletal muscle was the major site of virus replication at the early stage of infection, while the virus mainly accumulated in the brain at the late stage. In addition, susceptibility of mice to CA16 infection was found to be age dependent. Moreover, different CA16 strains could exhibit varied virulence *in vivo*. Importantly, we demonstrated that post-exposure treatment with an anti-CA16 monoclonal antibody fully protected mice against lethal CA16 infection. Collectively, these results indicate the successful development of a CA16 infection mouse model for anti-viral evaluation.

1. Introduction

Coxsackievirus A16 (CA16) and enterovirus 71 (EV71) are the two major causative agents of hand, foot, and mouth disease (HFMD) (Ang et al., 2009; Chatproedprai et al., 2010; Hosoya et al., 2007; Li et al., 2005; McMinn, 2002; Tu et al., 2007; Yang et al., 2011; Zhang et al., 2009), which is a common infectious disease in children under the age of 5 years (Wong et al., 2010). In general, patients infected with either EV71 or CA16 share common clinical manifestations, including skin rash, mucosal blister, sore throat, and fever. EV71 infections are often found to be associated with severe neurological complications, such as brainstem encephalitis, paralysis and pulmonary edema, and even death (McMinn, 2002; Solomon et al., 2010). Fatal cases of CA16 infection have been rarely reported (Goldberg and McAdams, 1963; Wang et al., 2004; Wright et al., 1963; Xu et al., 2012). However, recent clinical data demonstrate that CA16 infections also can cause severe neurological complications. For example, a recent clinical survey shows that 65 and 19 out of 92 HFMD patients with nervous system damage were infected with EV71 and CA16, respectively (Xu et al., 2012). Therefore, it is of major importance to understand further the pathogenesis of CA16 infection and to develop vaccines and therapeutic drugs against this infection.

Thus far, humans are the only known natural host of CA16. Development of a relevant small animal model of CA16 infection is thus critical for investigation of the mechanism of pathogenesis and for evaluation of vaccines and anti-viral agents. Recently, Mao et al. reported that intracerebral (i.c.) inoculation of neonatal mice with CA16 resulted in wasting, hind-limb paralysis, and even death (Mao et al., 2012). Our group also found that one-day-old mice could be infected with CA16 virus via the intraperitoneal (i.p.) route, leading to significant morbidity and mortality (Liu et al., 2012). In the present study, we further characterize this mouse model of CA16 infection and assess its utility in *in vivo* evaluation of anti-viral agents.

* Corresponding author. Address: Institut Pasteur of Shanghai, 320 Yueyang Road, Shanghai 200031, China. Tel.: +86 21 54923067; fax: +86 21 54923044.
E-mail address: huangzhong@ips.ac.cn (Z. Huang).
[1] These authors contributed equally to this paper.

http://dx.doi.org/10.1016/j.antiviral.2014.02.015
0166-3542/

2. Materials and methods

2.1. Cells and viruses

RD and Vero cells were grown in DMEM supplemented with 10% FBS, 100 U/ml penicillin and 100 μg/ml streptomycin, as described previously (Liu et al., 2011b). Two CA16 strains, CA16/SZ05 (GenBank ID: EU262658) (Wu et al., 2008; Yang et al., 2001) and CA16/G08 (GenBank ID: KC342228) (Liu et al., 2012), were propagated in RD cells. Virus titers were determined as described previously (Liu et al., 2011b).

2.2. Antibodies

Rabbit polyclonal antibody against CA16 VP1 protein was described previously (Liu et al., 2011b). Hepatitis B surface antigen-specific monoclonal antibody (mAb) 2G9 was described previously (Ku et al., 2012). Anti-CA16 neutralizing mAb 8C4 was generated in house from mice immunized with inactivated CA16 (unpublished results).

2.3. Mouse experiments

Groups of neonatal ICR mice were inoculated with 50 μl of CA16/SZ05 or CA16/G08 via the i.p. route. One group of mice was mock-infected with 50 μl of PBS via the same route and served as the control. After inoculation, the mice were monitored daily for survival and clinical manifestation for 2 or 3 weeks. Clinical scores were graded as follows: 0, healthy; 1, reduced mobility; 2, limb weakness; 3, paralysis; 4, death.

For anti-viral therapy experiments, we administered to mice a single dose (10 μg) of purified monoclonal antibody by i.p. injection at one day after infection. The treated mice were monitored daily for survival and clinical manifestation as described above.

All animal experiments described in this work were approved by the Institutional Animal Care and Use Committee at the Institut Pasteur of Shanghai, and the animals were cared for in accordance with the institutional guidelines.

2.4. Histopathology

Organs and tissues were harvested from euthanized mice and immediately fixed in 4% paraformaldehyde (Sigma) for 24 h at room temperature. After fixation, the tissues were paraffin embedded, sectioned, and stained with hematoxylin and eosin (H&E).

2.5. Immunohistochemical staining

Tissue sections were immerged in TBS buffer containing 3% acetic acid for 5 min at room temperature, boiled in 0.01 M citrate buffer (pH 6.0) for 15 min, and cooled down to room temperature. Then, the sections were blocked with 10% normal goat serum diluted in TBS buffer for 10 min at room temperature, incubated with a rabbit polyclonal antibody against CA16 VP1 protein (1:500 diluted) overnight at 4 °C, followed by incubation with AP-conjugated goat anti-rabbit IgG (1:1000 diluted) for 30 min at 37 °C. BCIP/NBT substrate (Promega) was applied to the sections for color development. The sections were also briefly stained with hematoxylin.

2.6. Real-time PCR

Total RNA was extracted from individual organs/tissues of infected mice using Trizol reagent (Invitrogen), and reverse transcribed using oligo(dT) primers and M-MLV reverse transcriptase

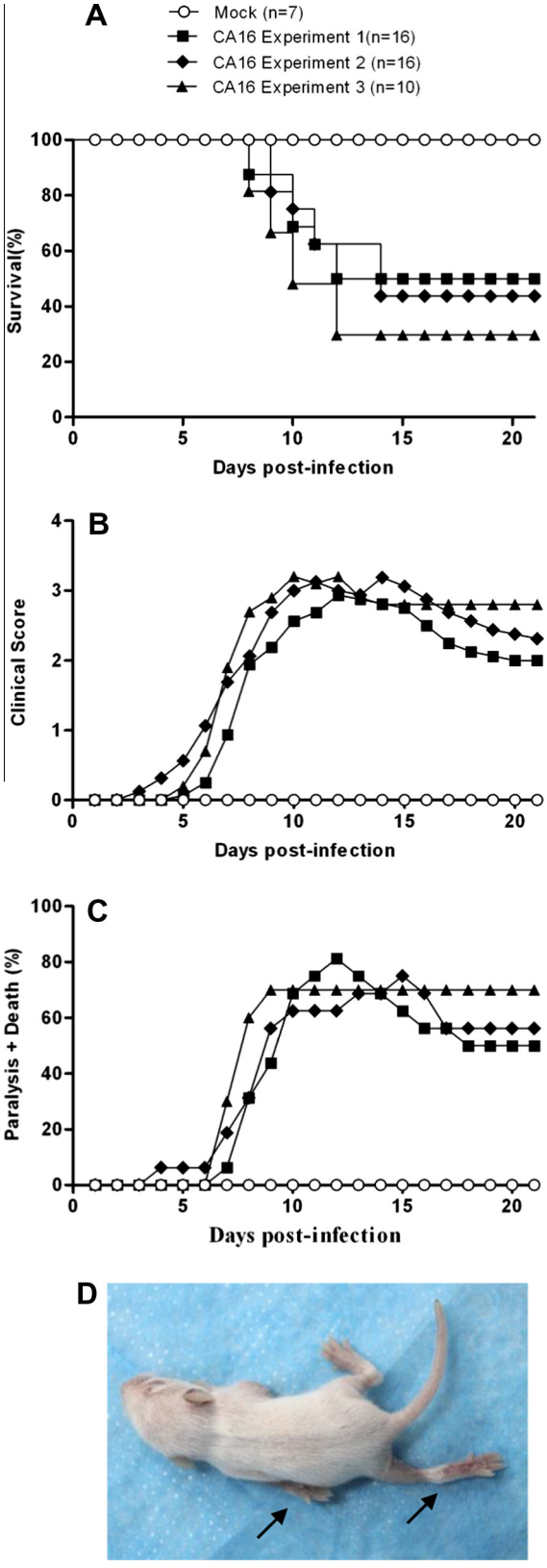

Fig. 1. One-day-old mice were susceptible to CA16 infection. Groups of 1-day-old ICR mice were inoculated i.p. with 2×10^6 TCID50 of CA16/SZ05 or with PBS. The inoculated mice were monitored daily for (A) survival and (B) clinical scores. Clinical scores were graded as follows: 0, healthy; 1, reduced mobility; 2, limb weakness; 3, paralysis; 4, death. (C) Percentage of mice exhibiting severe manifestations, including paralysis and death. (D) A mouse infected with CA16 exhibited limb paralysis (indicated by arrows).

Table 1
Summary of morbidity and mortality of mice infected with CA16/SZ05 at different ages.

Mouse age	CA16 dose	Total no. of mice	No. of mice exhibiting symptoms			No. of deaths
			Reduced mobility	Limb weakness	Paralysis	
1 day[§]	2×10^6	42	40 (95%)	40 (95%)	33 (79%)	24 (57%)
2 days	10^7	15	15 (100%)	15 (100%)	3 (20%)	2 (13%)[**]
7 days	10^7	13	1 (8%)	1 (8%)	1 (8%)	1 (8%)[**]

[§] Data are from three independent experiments.
[**] Significant difference ($P < 0.01$) between each age group and the 1-day-old group.

(Invitrogen) to produce cDNA, according to the manufacturer's instructions. The resultant cDNA was used for real-time PCR with a SYBR®Premix Ex Taq™ kit (TaKaRa) and primers (forward 5′-ATCCAGTAAGGATCCCAGACT-3′ and reverse 5′-GATTTGCATAGTGGAGAGCAG-3′). Plasmid pMD19-CV (Liu et al., 2011a) was used as standard for quantification of copy numbers. Real-time PCR reactions were carried out for 40 cycles of 95 °C for 15 s and 60 °C for 30 s in a 7900HT Fast Real-Time PCR System (Applied Biosystems).

2.7. Statistical analysis

All statistical analysis was performed with GraphPad Prism version 5. Kaplan–Meier survival curves were compared by the log-rank test. A two-tailed *P* value of <0.05 was considered statistically significant.

3. Results

3.1. One-day-old mice infected with CA16 developed neurological complications and death

We first examined whether neonatal mice were susceptible to CA16 infection. One-day-old ICR mice were injected i.p. with 2×10^6 TCID50 of the CA16/SZ05 strain and then observed for clinical signs on a daily base for 21 days. The results of three independent experiments are summarized in Fig. 1. CA16-inoculated mice started to die at 8 days post-infection (dpi) and all the deaths occurred within the second week (8–14 dpi). The survival rates ranged from 50% to 30% at the end of the experiments (Fig. 1A). During the course, CA16-infected mice showed clinical signs, such as reduced mobility, and limb weakness and paralysis (Table 1, Fig. 1B–D) before death. In contrast, mock-infected mice appeared to be healthy throughout the course (Fig. 1A–C).

To determine the cause of paralysis and death, brain, intestine and hind limbs from CA16-infected mice in the moribund state or from age-matched naïve mice were subjected to histopathological examination. The control mice did not show any abnormality in the tissues examined (Fig. 2A, 2C and 2E). In contrast, neuronal degeneration and loss in the brainstem (Fig. 2B), necrotizing myositis with inflammatory infiltration in the limb muscles (Fig. 2D), and massive villous damage in the small intestines (Fig. 2F), were observed in the CA16-infected mice. Immunohistochemical staining using a CA16 VP1-specific antibody revealed the presence of the viral protein in the brainstem of the CA16-infected mice (Fig. 2H).

3.2. Distribution and replication of CA16 in tissues

To determine how CA16 spreads and replicates *in vivo* upon inoculation, the virus load in the blood, heart, liver, lungs, spleens, brain, intestines and limb muscles of CA16-infected mice was measured by real-time PCR. As shown in Fig. 3, at an early stage of infection (3 dpi), virus was detected in all the organs/tissues

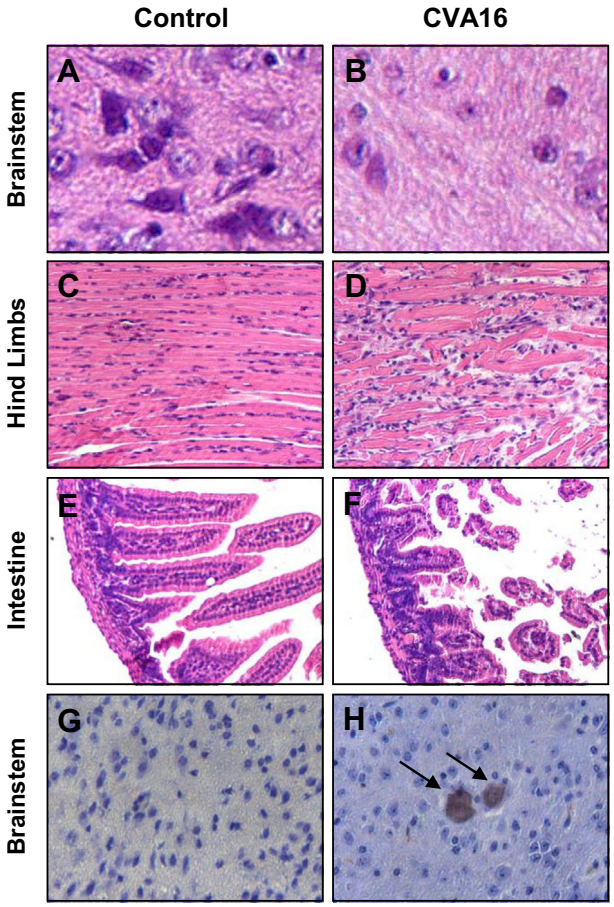

Fig. 2. Histological examination of CA16-infected mice. Groups of 1-day-old ICR mice were inoculated i.p. with PBS (A, C, E and G) or 2×10^6 TCID50 of CA16 (B, D, F and H). Tissues from the animals were subjected to H&E staining (A–F) or immunohistochemical staining with a CA16 VP1-specific antibody followed by brief hematoxylin staining (G and H). Data shown are representative of three mice in each group with similar histologies.

assayed, except that virus in the blood was barely detectable (note that $<10^3$ copies/mg tissue or μl blood was considered negative). The limb muscles contained the highest virus titer at 3 and 6 dpi, indicating that skeletal muscle is the major site of early viral replication. In general, from 6 to 9 dpi virus load showed a decreasing trend for all organs/tissues except the brain. Indeed, viral RNA in the brain at 9 dpi increased by 1 log as compared to that at 6 dpi, suggesting the virus spread to and replicated in the brain at a relatively late stage of infection (Fig. 3).

3.3. Age-dependent susceptibility of mice to CA16/SZ05 infection

Two- and seven-day-old ICR mice were compared for susceptibility to CA16 infection. After i.p. inoculation with 10^7 TCID50

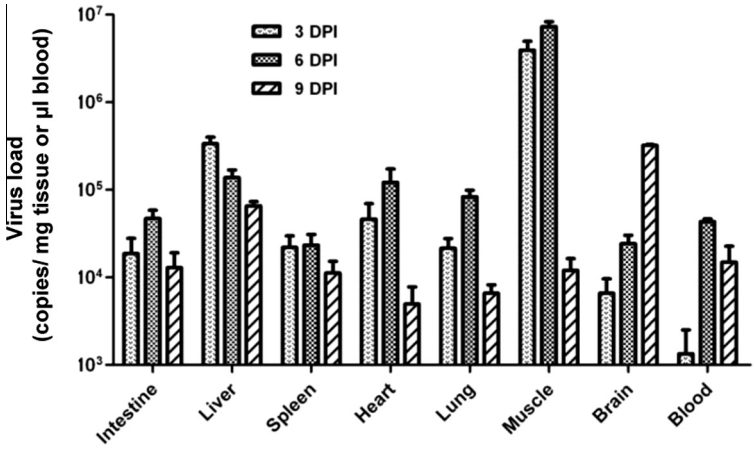

Fig. 3. Virus titers in organs from mice infected with CA16. One-day-old ICR mice were inoculated i.p. with the CA16/SZ05 at 2×10^6 TCID50/mouse. At 3, 6 and 9 dpi, mice ($n = 3$) were euthanized, and virus titers in the indicated organs/tissues were determined by real time RT-PCR. Results are expressed as viral RNA copies/mg tissue or μl blood. Data represent the means ± SEM of results of three mice.

CA16, both groups of infected mice had a low fatality rate, with only one death in each group (Table 1 and Fig. 4). However, the clinical outcome for the two groups was significantly different. Mice in the 2-day-old group started to develop severe clinical signs at ~7 dpi (Fig. 4B), and during the course of observation, 100% and 20% of the mice showed limb weakness and paralysis, respectively (Table 1). In contrast, only one out of 13 (8%) mice in the 7-day-old group exhibited reduced mobility at 10 dpi (Fig. 4B), and eventually developed limb weakness and paralysis and died (Table 1). These results indicate that age is a limiting factor for efficient CA16 infection in mice.

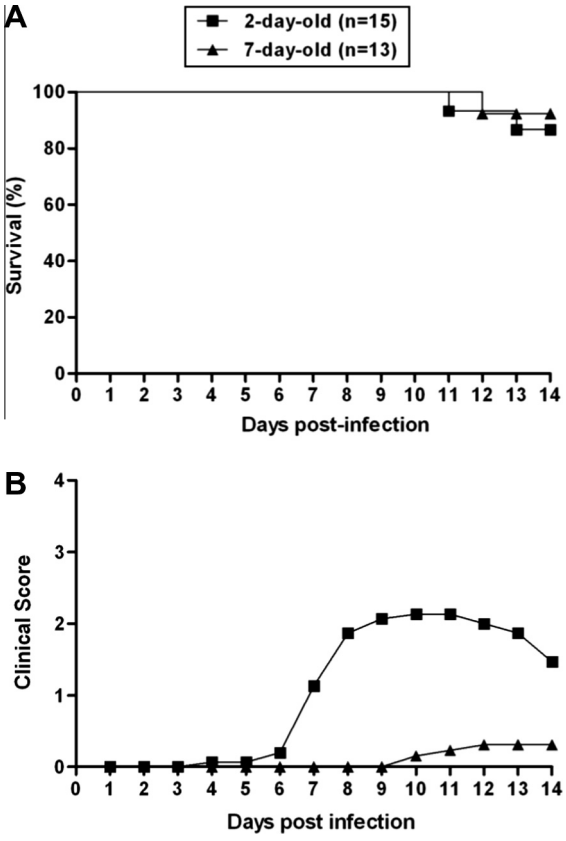

Fig. 4. Clinical outcome of CA16 inoculation of mice of different ages. One group of 2-day-old ICR mice ($n = 15$) and another group of 7-day-old ICR mice ($n = 13$) were inoculated i.p. with 10^7 TCID50 of CA16, and then monitored daily for (A) survival and (B) clinical scores. Clinical scores were graded as follows: 0, healthy; 1, reduced mobility; 2, limb weakness; 3, paralysis; 4, death.

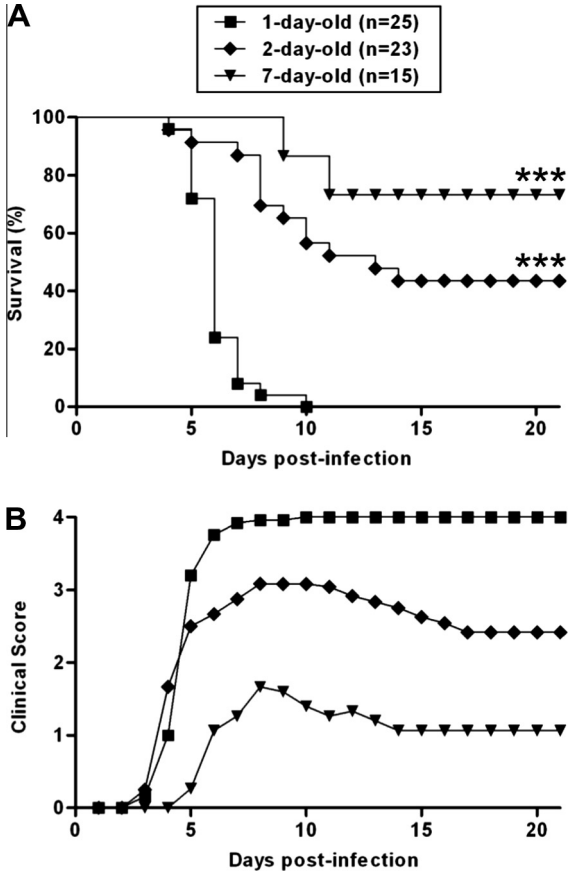

Fig. 5. *In vivo* virulence of the CA16/G08 strain. ICR mice at age of 1-day-old ($n = 25$), 2-day-old ($n = 23$) or 7-day-old ($n = 15$) were inoculated i.p. with 1.4×10^6 TCID50 of CA16/G08, and then monitored daily for (A) survival and (B) clinical scores. Clinical scores were graded as follows: 0, healthy; 1, reduced mobility; 2, limb weakness; 3, paralysis; 4, death. The logrank test was used to compare the survival rate between each age group and the 1-day-old group. *** indicate significant differences ($P < 0.001$).

3.4. In vivo virulence of the CA16/G08 strain

Another clinical isolate CA16/G08 was also tested for its infectivity in 1-, 2-, or 7-day-old mice. As shown in Fig. 5, i.p. inoculation with 1.4×10^6 TCID50 of CA16/G08 resulted in 100%, 56% and 26.7% mortality for the 1-, 2- and 7-day-old mouse groups, respectively. These mortality rates are much higher than those (57%, 13% and 8% for the corresponding age groups, respectively) caused by CA16/SZ05 infection (Table 1). These data indicate that CA16/G08 is more virulent *in vivo* than CA16/SZ05.

3.5. Evaluation of the therapeutic efficacy of anti-CA16 monoclonal antibody in the mouse model

The utility of the mouse model in evaluation of anti-viral agents was assessed using mAbs. Neonatal mice were i.p. inoculated with 2.7×10^5 TCID50 of CA16/G08 and one day later administered via the i.p. route with PBS, a single dose (10 μg) of anti-CA16 mAb 8C4 or irrelevant anti-HBsAg mAb 2G9 as control. As shown in Fig. 6, mice receiving PBS or the control mAb gradually developed severe diseases, resulting in more than 60% mortality; in contrast, all the 8C4-treated mice survived without showing clinical signs.

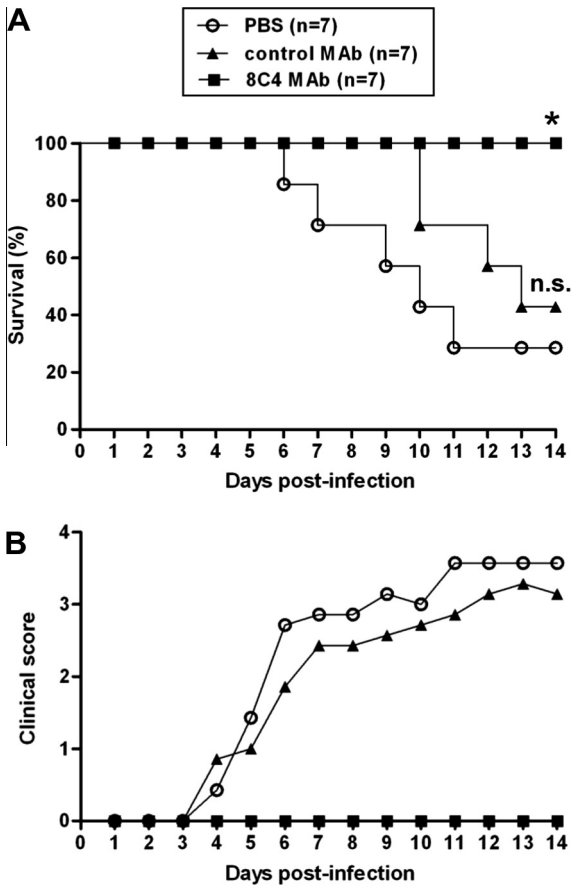

Fig. 6. Therapeutic effect of monoclonal antibody treatment in the CA16 infection mouse model. Three groups of 2-day-old ICR mice were inoculated i.p. with 2.7×10^5 TCID50 of CA16/G08, and one day later administered i.p. with PBS, 10 μg of anti-CA16 mAb 8C4, or 10 μg of control mAb 2G9, respectively. The treated mice were observed daily for (A) survival and (B) clinical scores. Clinical scores were graded as follows: 0, healthy; 1, reduced mobility; 2, limb weakness; 3, paralysis; 4, death. The logrank test was used to compare the survival rate between each treatment group and the PBS control group. Statistical significance is indicated as follows: n.s., $P > 0.05$; *, $P < 0.05$.

4. Discussion and conclusion

CA16 is known to naturally infect humans only. It is thus important to develop a small animal model of CA16 infection to facilitate the study of mechanisms of CA16 infection and the development of CA16 vaccines and therapeutic drugs. Previously, it was reported that neonatal mice could be infected by CA16 through i.c. inoculation, resulting in severe morbidity and mortality, and that passive transferred anti-CA16 neutralizing sera provided protection against CA16 challenge in this mouse model (Mao et al., 2012). However, the use of this model requires careful handling and extreme preciseness in performing i.c. injection, and therefore may not be widely applicable. As compared to the i.c. route, i.p. inoculation is an easier and more common practice. In the present study, we showed that i.p. inoculation of 1- or 2-day-old ICR mice led to severe clinical manifestations, including limb paralysis, and death. Virus was detected in many organs/tissues, including the brain, of the infected mice. These data demonstrate that i.p. inoculation of CA16 could establish productive infection in neonatal mice. Using this mouse model of CA16 infection, our group recently showed that passive transfer of CA16-VLP immunized sera protected recipient neonatal mice against lethal CA16 infection (Liu et al., 2012), demonstrating the protective efficacy of the candidate vaccine. In the present study, we showed that post-infection treatment with anti-CA16 mAb 8C4 fully protected mice from disease (Fig. 6) and thus identified 8C4 as an elite candidate for therapeutic drug development. Together, these results indicate the successful development of a simple, easily handled animal model of CA16 infection, which is valuable in assessing the *in vivo* efficacy of anti-CA16 vaccines and therapeutic drugs.

Patients infected with CA16 usually display mild clinical signs, such as fever, rash and mucosal ulcers. A small proportion of patients may develop severe complications, such as myocarditis (Wang et al., 2004), brainstem encephalitis and acute flaccid paralysis (Xu et al., 2012), suggesting the involvement of the central nervous system (CNS) in disease development. In the CA16-infected mice, the virus load of the limb muscles was the highest among the tested tissues at 3 and 6 dpi, but decreased by more than 2 log at 9 dpi, indicating that limb muscle is the major site for early- but not late-stage virus replication (Fig. 3); immunohistological examination further confirmed the presence of CA16 in the limb muscles (data not shown). In contrast, the virus titer in the brain increased progressively and peaked at 9 dpi (Fig. 3), strongly suggesting that CA16 is neurotropic. Indeed, the presence of virus in the CNS was demonstrated by immunohistochemistry (Fig. 2H). CA16 infection resulted in significant neuronal damage in the brainstem (Fig. 2B). For the CA16-infected mice, the incident rate of paralysis/death increased rapidly at around 9 dpi, when the virus titers in the brain were much higher than that in the limb muscle (Fig. 1C and 3). Therefore, it was likely that the limb paralysis observed in the CA16-infected mice was of neurogenic origin, rather than due to limb muscle damage. However, one cannot rule out the possibility that myositis may partially have contributed to the observed paralysis and/or death.

In summary, our results not only demonstrate the successful development of a mouse model of CA16 infection for evaluation of vaccines and anti-viral agents, but also shed light on the pathogenesis of CA16-induced disease.

Acknowledgements

We thank Drs. Bing Sun and Qi Jin for providing the CA16 virus. This work was supported by grants from the National Natural Science Foundation of China (31370930), the Science and Technology Commission of Shanghai Municipality (13431900601,

13ZR1462900), and the Chinese Academy of Sciences "100 Talents" program (#KSCX2-YW-BR-2). Q.L. was partly supported by a Post-doc Fellowship grant from the Shanghai Institutes for Biological Science (SIBS), Chinese Academy of Sciences. Q.L. and Z.H. gratefully acknowledges the support of SA-SIBS scholarship program.

References

Ang, L.W., Koh, B.K., Chan, K.P., Chua, L.T., James, L., Goh, K.T., 2009. Epidemiology and control of hand, foot and mouth disease in Singapore, 2001–2007. Ann. Acad. Med. Singapore 38, 106–112.

Chatproedprai, S., Theanboonlers, A., Korkong, S., Thongmee, C., Wananukul, S., Poovorawan, Y., 2010. Clinical and molecular characterization of hand-foot-and-mouth disease in Thailand, 2008–2009. Jpn. J. Infect. Dis. 63, 229–233.

Goldberg, M.F., McAdams, A.J., 1963. Myocarditis possibly due to coxsackie group A, type 16, virus. J. Pediatr. 62, 762–765.

Hosoya, M., Kawasaki, Y., Sato, M., Honzumi, K., Hayashi, A., Hiroshima, T., Ishiko, H., Kato, K., Suzuki, H., 2007. Genetic diversity of coxsackievirus A16 associated with hand, foot, and mouth disease epidemics in Japan from 1983 to 2003. J. Clin. Microbiol. 45, 112–120.

Ku, Z., Shi, J., Liu, Q., Huang, Z., 2012. Development of murine monoclonal antibodies with potent neutralization effects on enterovirus 71. J. Virol. Methods 186, 193–197.

Li, L., He, Y., Yang, H., Zhu, J., Xu, X., Dong, J., Zhu, Y., Jin, Q., 2005. Genetic characteristics of human enterovirus 71 and coxsackievirus A16 circulating from 1999 to 2004 in Shenzhen, People's Republic of China. J. Clin. Microbiol. 43, 3835–3839.

Liu, F., Liu, Q., Cai, Y., Leng, Q., Huang, Z., 2011a. Construction and characterization of an infectious clone of coxsackievirus A16. Virol. J. 8, 534.

Liu, Q., Ku, Z., Cai, Y., Sun, B., Leng, Q., Huang, Z., 2011b. Detection, characterization and quantitation of coxsackievirus A16 using polyclonal antibodies against recombinant capsid subunit proteins. J. Virol. Methods 173, 115–120.

Liu, Q., Yan, K., Feng, Y., Huang, X., Ku, Z., Cai, Y., Liu, F., Shi, J., Huang, Z., 2012. A virus-like particle vaccine for coxsackievirus A16 potently elicits neutralizing antibodies that protect mice against lethal challenge. Vaccine 30, 6642–6648.

Mao, Q., Wang, Y., Gao, R., Shao, J., Yao, X., Lang, S., Wang, C., Mao, P., Liang, Z., Wang, J., 2012. A neonatal mouse model of coxsackievirus A16 for vaccine evaluation. J. Virol. 86, 11967–11976.

McMinn, P.C., 2002. An overview of the evolution of enterovirus 71 and its clinical and public health significance. FEMS Microbiol. Rev. 26, 91–107.

Solomon, T., Lewthwaite, P., Perera, D., Cardosa, M.J., McMinn, P., Ooi, M.H., 2010. Virology, epidemiology, pathogenesis, and control of enterovirus 71. Lancet Infect. Dis. 10, 778–790.

Tu, P.V., Thao, N.T., Perera, D., Huu, T.K., Tien, N.T., Thuong, T.C., How, O.M., Cardosa, M.J., McMinn, P.C., 2007. Epidemiologic and virologic investigation of hand, foot, and mouth disease, southern Vietnam, 2005. Emerg. Infect. Dis. 13, 1733–1741.

Wang, C.Y., Li Lu, F., Wu, M.H., Lee, C.Y., Huang, L.M., 2004. Fatal coxsackievirus A16 infection. Pediatr. Infect. Dis. J. 23, 275–276.

Wong, S.S., Yip, C.C., Lau, S.K., Yuen, K.Y., 2010. Human enterovirus 71 and hand, foot and mouth disease. Epidemiol. Infect. 138, 1071–1089.

Wright Jr., H.T., Landing, B.H., Lennette, E.H., Mc, A.R., 1963. Fatal infection in an infant associated with coxsackie virus group A, type 16. N. Engl. J. Med. 268, 1041–1044.

Wu, Z., Gao, Y., Sun, L., Tien, P., Jin, Q., 2008. Quick identification of effective small interfering RNAs that inhibit the replication of coxsackievirus A16. Antiviral Res. 80, 295–301.

Xu, W., Liu, C.F., Yan, L., Li, J.J., Wang, L.J., Qi, Y., Cheng, R.B., Xiong, X.Y., 2012. Distribution of enteroviruses in hospitalized children with hand, foot and mouth disease and relationship between pathogens and nervous system complications. Virol. J. 9, 8.

Yang, F., Jin, Q., He, Y., Li, L., Hou, Y., 2001. The complete genome of enterovirus 71 China strain. Sci. China C. Life Sci. 44, 178–183.

Yang, F., Zhang, T., Hu, Y., Wang, X., Du, J., Li, Y., Sun, S., Sun, X., Li, Z., Jin, Q., 2011. Survey of enterovirus infections from hand, foot and mouth disease outbreak in China, 2009. Virol. J. 8, 508.

Zhang, Y., Tan, X.J., Wang, H.Y., Yan, D.M., Zhu, S.L., Wang, D.Y., Ji, F., Wang, X.J., Gao, Y.J., Chen, L., An, H.Q., Li, D.X., Wang, S.W., Xu, A.Q., Wang, Z.J., Xu, W.B., 2009. An outbreak of hand, foot, and mouth disease associated with subgenotype C4 of human enterovirus 71 in Shandong, China. J. Clin. Virol. 44, 262–267.